

Influence of the Heat Transfer on Dynamic Properties of Mesoscopic Superconducting Strips: A Finite Element Method

YAJING WANG^a, LIN PENG^{a,*}, JIA LIN^a, YUFENG ZHANG^a AND LINA SANG^b

^aDepartment of Physics, Shanghai University of Electric Power, Shanghai 201300, China

^bInstitute for Superconducting and Electronic Materials, Faculty of Engineering,

Australian Institute for Innovative Materials, University of Wollongong, NSW 2500, Australia

(Received November 24, 2019; revised version January 11, 2020; in final form January 29, 2020)

Using a finite element method to numerically solve the time-dependent Ginzburg–Landau equations, we studied the dynamic properties of the mesoscopic superconducting strips. We obtain the different voltage–current, free energy–time, and vortex evolution patterns for different temperatures conditions and applied current. Our results show that the temperature and the applied current directly influence the dynamics of the superconducting condensate and lead to the variations of threshold current and the periodic oscillations of the free energy across the strips with a frequency.

DOI: [10.12693/APhysPolA.137.1116](https://doi.org/10.12693/APhysPolA.137.1116)

PACS/topics: threshold current, periodic oscillations, time-dependent Ginzburg–Landau equations, finite element method

1. Introduction

In the last decade superconductivity at decreased structure dimensions has received an increasing interest mainly due to the huge advancements in modern nanofabrication techniques. Mesoscopic superconductors constitute a class of materials where size effects can play a relevant role to determine the vortex arrangement throughout the superconducting film [1–12]. When their thickness is much smaller than the coherence length ξ and the penetration depth λ , the external magnetic field in terms of vortices can penetrate into a superconducting film, and vortex interactions with other vortices and with the screening currents circulating around the edges give rise to a variety of configurations, such as the giant vortex state [7, 8], multivortex state [9, 10], and vortex-antivortex state [11, 12]. Meanwhile, the magnetic flux vortex configurations are strongly influenced by both the geometry and size of the sample [13]. The physics becomes even richer when an electric field is applied to these samples in addition to a magnetic field, resulting in the phase-slip phenomenon and oscillatory phenomena [2, 14]. For example, a superconducting strip with a perpendicular magnetized dots on top in the presence of an applied dc current exhibits the periodic oscillations of the voltage due to the phase-slip phenomenon [2]. The mesoscopic superconducting weak links indicate possible magnetoresistance oscillations and reentrance of superconductivity due to the current driven transition from the Abrikosov–Josephson to Josephson-like vortex [14].

Oscillatory phenomena, which are an important part of the electronic scene, are readily found in nonequilibrium superconductivity. However, mesoscopic superconducting film may also exhibit oscillation features, such as free energy and amplitude of the voltage oscillation. In this paper, we study the dynamic properties of the mesoscopic superconducting strips under the influences of temperature, applied current, and applied magnetic fields, and investigate the possible oscillation phenomenon. Numerical simulations are performed inside the framework of the time-dependent Ginzburg–Landau (TDGL) model. Also, by using finite-element method (FEM) [15, 16], the TDGL equations are numerically solved to obtain the dynamic properties of the superconducting strips.

The work is organized as follows. In Sect. 2, we show the derived TDGL equations and explain the numerical method and procedure used in the calculations. In Sect. 3, we analyze the results obtained for the superconducting strips. Our results are finally summarized in Sect. 4.

2. Theoretical formalism

We consider a mesoscopic superconducting stripe and the superconducting state is usually described by the complex order parameter ψ . The quantity $|\psi|^2$ represents the electronic density of the Cooper pairs. In the regions where $|\psi|^2$ is small, superconductivity is suppressed. At the center of the vortex $|\psi|^2 = 0$, whereas the local magnetic field \mathbf{B} is maximum. We restrict ourselves to a sufficiently thin strip such that the thickness $d \ll \xi, \lambda$ (ξ is the coherence length, λ is the penetration depth). The strip is surrounded by vacuum with an applied magnetic field $\mathbf{H} = (0, 0, H)$ in the z -direction and the transport current $\mathbf{I} = (0, I, 0)$ in the y -direction. The order

*corresponding author; e-mail: plpeng@shiep.edu.cn

parameter and the local magnetic field can be determined by the Ginzburg–Landau (GL) equations in their time-dependent formalism, expressed by [17]:

$$\left(\frac{\partial}{\partial t} + i\Phi\right)\psi = (\nabla - i\mathbf{A})^2\psi + (1 - T - |\psi|^2)\psi, \quad (1)$$

$$\sigma\left(\frac{\partial\mathbf{A}}{\partial t} + \nabla\Phi\right) =$$

$$\text{Re}[\psi^*(-i\nabla - \mathbf{A})\psi] - \kappa^2\nabla \times \nabla \times \mathbf{A}, \quad (2)$$

where Φ is the scalar potential, ψ is the complex order parameter, \mathbf{A} is vector potential, κ is GL parameter, and σ is the conductivity constant. The first equation governs the relaxation of the superconducting order parameter ψ , and the second equation is the Maxwell equation for the induced magnetic field $\mathbf{B} = \nabla \times \mathbf{A}$. All physical quantities are measured in dimensionless units. The distances are scaled with the coherence length $\xi(0)$. \mathbf{A} is given in units of $\Phi_0/2\pi\xi(0)$ ($\Phi_0 = ch/2e$ is the flux quantum). The magnetic field is in units of $H_{c2} = \Phi_0/2\pi\xi(0)^2 = \sqrt{2}\kappa H_c$, where H_c is the thermodynamic critical field and $\kappa = \lambda/\xi$ is the GL parameter. The time is in units of GL relaxation time $t_0 = \pi\hbar/8k_B T_c$. Temperature T is in units of T_c (critical temperature). Order parameter ψ is scaled to its value at zero magnetic field. The free energy of the superconducting state, measured in $F_0 = H_c^2 V/8\pi$ units, is expressed as

$$F = \frac{2}{V} \int \left[-|\psi|^2 + \frac{1}{2}|\psi|^4 + |(\nabla - i\mathbf{A})\psi|^2 + \kappa^2(\nabla \times \mathbf{A} - \mathbf{H})^2 \right] dV. \quad (3)$$

To account for heating effects, we couple Eq. (1) and Eq. (2) to the heat transfer equation

$$\nu \frac{\partial T}{\partial t} = \zeta \nabla^2 T + \left(\frac{\partial \mathbf{A}}{\partial t}\right)^2 - \eta(T - T_0), \quad (4)$$

where T_0 is the bath temperature. Here we use $\nu = 0.03$, $\zeta = 0.06$, and $\eta = 2 \times 10^{-4}$, corresponding to an intermediate heat removal to the substrate [18]. The transport current is introduced via the boundary condition for the vector potential $\nabla \times \mathbf{A}|_z(x=0, w) = H \pm H_I$. The external dc current I is induced by imposed H_I on the lateral edges of the sample. From the vector potential it is possible to obtain the voltage by using the relation $V = \frac{\partial}{\partial t} \int \mathbf{A} dl$. The applied current is given in units of $j_0 = \sigma_n \hbar/2et_0 \xi(0)$ (σ_n is the normal-state conductivity), and the voltage scale is given by $V_0 = \hbar/2et_0$.

For the magnetic field, the boundary condition reads: $(\nabla \times \mathbf{A})|_{\text{boundary}} = \mathbf{H}$. For the order parameter, we use the superconductor-insulator boundary conditions, i.e., we set the normal component of the supercurrent across the boundary to zero: $\mathbf{n} \cdot (\nabla - i\mathbf{A})\psi|_{\text{boundary}} = 0$, where \mathbf{n} is the outward normal unit to the surface. Finally, to simulate a infinite length strip, we apply periodic boundary conditions in the y -direction: $\psi(x, y) = \psi(x, y + L_y)$ and $\mathbf{A}(x, y) = \mathbf{A}(x, y + L_y)$, where L_y is the length of the simulated rectangular unit cell (with width L_x).

The TDGL equations and their discrete forms are gauge invariant under the transformations as follows: $\psi' = \psi e^{i\chi}$, $\mathbf{A}' = \mathbf{A} + \nabla\chi$, $\Phi' = \Phi - \partial\chi/\partial t$. We chose the zero-scalar potential gauge, that is, $\Phi = 0$ at all times and positions.

3. Results and discussions

We first consider the mesoscopic superconducting strip with sizes of $L_x = 5\xi$ and $L_y = 11\xi$. Our simulations have been carried out by using $\sigma = 1$ and $\kappa = 1.2$ for the superconducting strip. The initial conditions are $|\psi|^2 = 1$ corresponding to the Meissner state and zero magnetic field inside the superconductor. Figure 1 shows the time-averaged voltage as a function of the applied current ($V(I)$) in the superconducting strip at $H/H_{c2} = 0.2$, $T/T_c = 0.85$. It is known that the superconducting strip goes through two levels of increasing resistance as driving current is increased. Low resistance of the superconducting strip is maintained up to a threshold current when maximal current in the strip reaches the de-pairing current. The threshold current is $I_c/I_0 = 0.006$. With further increase in applied current, superconductivity becomes utterly suppressed in the strip, leading to a normal state of higher resistance.

Figure 2 shows free energy as a function of the time ($F(t)$) at $H/H_{c2} = 0.2$, $T/T_c = 0.85$, and $I/I_0 = 0.005$, which indicates the period $\tau/t_0 \approx 1400$ of the free-energy oscillation. The inset shows the contour plots of the Cooper-pair density at the corresponding time. Under the drive of the applied current, vortices move along the y -axis.

Figure 3 shows the time-averaged voltage as a function of the applied current in the superconducting strip at $H/H_{c2} = 0.6$ for the $T/T_c = 0.5, 0.3$, and 0.1 , respectively. We observed that the corresponding threshold

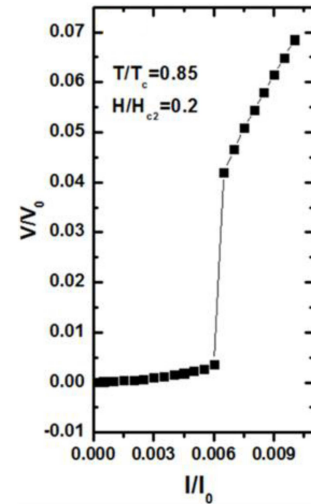


Fig. 1. The time-averaged voltage as a function of the applied current in the superconducting strip with dimensions $L_x = 5\xi$ and $L_y = 11\xi$ at $H/H_{c2} = 0.2$, $T/T_c = 0.85$.

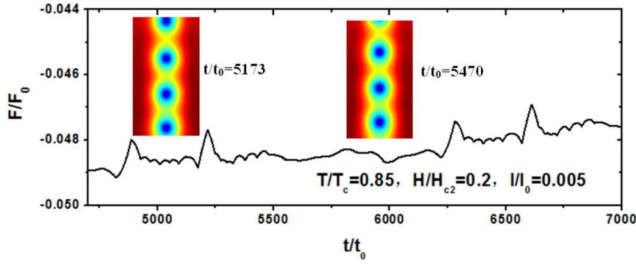


Fig. 2. Free energy vs. time characteristics of the strip at $H/H_{c2} = 0.2$, $T/T_c = 0.85$ and $I/I_0 = 0.005$. The inset shows the contour plots of the Cooper-pair density at the corresponding time. Blue to red means that the absolute value of the order parameter ranges from minimum to maximum.

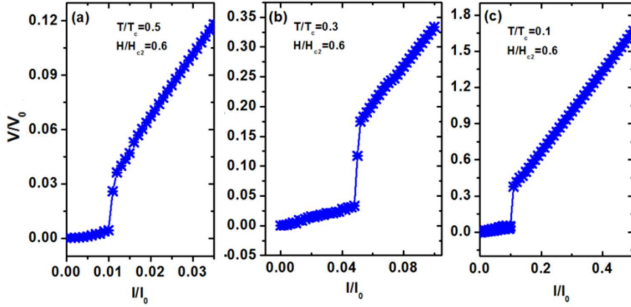


Fig. 3. (a)–(c) The time-averaged voltage as a function of the applied current in the superconducting strip with dimensions $L_x = 5\xi$ and $L_y = 11\xi$ at $H/H_{c2} = 0.6$ for the $T/T_c = 0.5, 0.3$, and 0.1 , respectively.

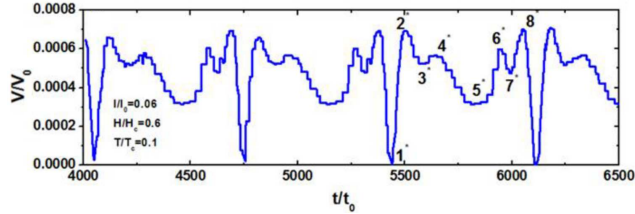


Fig. 4. Voltage vs. time characteristics of the strip at $H/H_c = 0.6$, $I/I_0 = 0.06$ and $T/T_c = 0.1$.

currents were $I_c/I_0 = 0.01, 0.05$ and 0.1 , respectively. With decrease in temperature T , the threshold current increases. Figure 4 shows voltage vs. time characteristics $V(t)$ of the strip at $H/H_c = 0.6$, $I/I_0 = 0.06$, and $T/T_c = 0.1$, which indicates the period $\tau/t_0 \approx 680$ of the voltage oscillation.

For the chosen length of simulation region and the considered magnetic field, we actually had $N_v = 2$ vortices moving in a single row, as shown in the contour plots of the Cooper-pair density in Fig. 5. There, points 1–8 are used to denote one period of the vortex dynamics, making the characteristic instance. The $V(t)$ characteristic

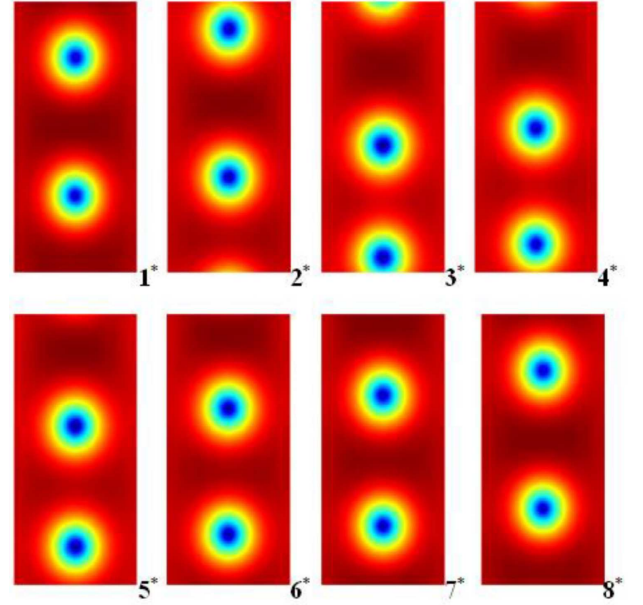


Fig. 5. Contour plots of the Cooper-pair density at time intervals indicated in Fig. 3b. Blue to red means that the absolute value of the order parameter ranges from minimum to maximum.

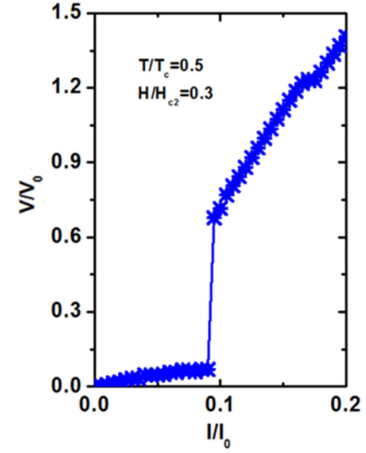


Fig. 6. The time-averaged voltage as a function of the applied current in the superconducting strip with dimensions $L_x = 10\xi$ and $L_y = 21\xi$ at $H/H_{c2} = 0.3$ and $T/T_c = 0.5$.

shows periodic oscillations with a minima corresponding to the entry of a vortex row inside the strip (see the cycle-*1). At a later time the new vortex would enter into the strip from the down boundary (cycle-*2) and pushes the previous one out of the strip, which leads to a maximum in the voltage. Subsequently, the new vortex interacts with the previous vortex (cycle-*3, *4, *5, *6, *7, *8). Ultimately, the superconducting condensate relaxes towards its minimum.

Up to now we studied the dynamic properties of the superconducting strip with dimensions $L_x = 5\xi$ and $L_y = 11\xi$. In what follows, we consider a superconducting

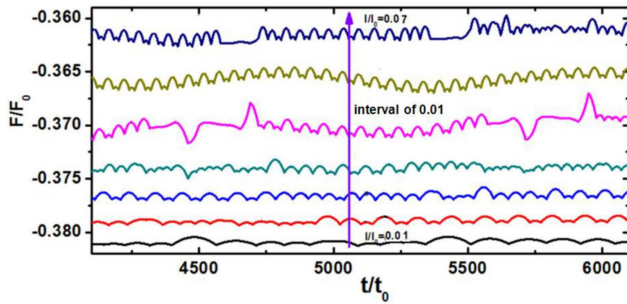


Fig. 7. Free-energy vs. time characteristics in the superconducting strip with dimensions $L_x = 10\xi$ and $L_y = 21\xi$ at $H/H_{c2} = 0.3$, $T/T_c = 0.5$ for the $I/I_0 = 0.01, 0.02, \dots, 0.07$ (interval of 0.01).

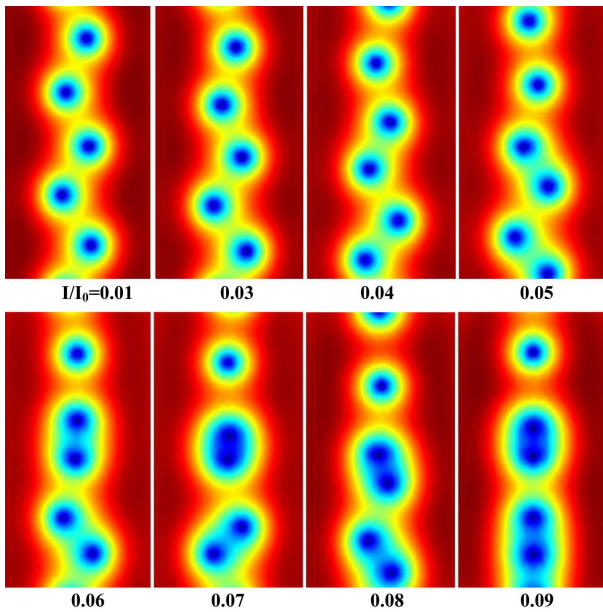


Fig. 8. Contour plots of the Cooper-pair density at the $I/I_0 = 0.01, 0.03, 0.04, 0.05, 0.06, 0.07, 0.08, 0.09$ (time-steps: 5000). Blue to red means that the absolute value of the order parameter ranges from minimum to maximum.

strip with dimensions $L_x = 10\xi$ and $L_y = 21\xi$. Figure 6 shows the time-averaged voltage as a function of the applied current in the superconducting strip at $H/H_{c2} = 0.3$ and $T/T_c = 0.5$. We observed that the threshold current was $I_c/I_0 = 0.09$.

Figure 7 shows free-energy vs. time characteristics in the superconducting strip at $H/H_{c2} = 0.3$ and $T/T_c = 0.5$ for the $I/I_0 = 0.01, 0.02, \dots, 0.07$ (interval of 0.01). When $I/I_0 < 0.05$, the free energy curves exhibit a similar oscillation behavior, which indicates the similar vortex motion (see Fig. 8). When $I/I_0 \geq 0.05$, we observed the multi-harmonic free-energy oscillation phenomenon and the asymmetric distribution of the vortices (see Fig. 8). Maybe we can understand this phenomenon in the following way. The vortex entering into the strip breaks the symmetry of the flow of the current in the

strip, and breaks the symmetry of the positions of the vortices, which leads to the multi-harmonic oscillation of free energy shown in Fig. 7. That suggests that the corresponding free-energy oscillates out of phase with its own frequency tunable both by the applied current and by the temperature.

4. Conclusions

In conclusion, using the TDGL theory we studied the dynamic properties of the mesoscopic superconducting strips at different temperatures. Through our research, the dynamic properties of two different sizes of superconducting strips were obtained. On the one hand, we obtained the corresponding threshold currents for the superconducting strip with dimensions $L_x = 5\xi$ and $L_y = 11\xi$. On the other hand, the multi-harmonic oscillation of free energy was found for the superconducting strip with dimensions $L_x = 10\xi$ and $L_y = 21\xi$. The free energy oscillates out of phase with its own frequency, which is attributed to the influences of both the temperature and the applied current on the vortices in the superconducting strip.

Acknowledgments

This work is sponsored by the National Natural Science Foundation of China (61875119), Shanghai Rising-Star Program (Grant No. 19QA1404000) and the Natural Science Foundation of Shanghai (No. 17ZR1411400).

References

- [1] M.V. Milošević, G.R. Berdiyrov, F.M. Peeters, *Phys. Rev. Lett.* **95**, 147004 (2005).
- [2] G.R. Berdiyrov, M.V. Milošević, F.M. Peeters, *Phys. Rev. B* **80**, 214509 (2009).
- [3] M. Iavarone, A. Scarfato, F. Bobba, M. Longobardi, G. Karapetrov, V. Novosad, V. Yefremenko, F. Giubileo, A.M. Cucolo, *Phys. Rev. B* **84**, 024506 (2011).
- [4] P. Sabatino, G. Carapella, G. Costabile, *Supercond. Sci. Technol.* **24**, 125007 (2011).
- [5] G. Carapella, P. Sabatino, G. Costabile, *Phys. Rev. B* **81**, 054503 (2010).
- [6] D.A. Frota, A. Chaves, W.P. Ferreira, G.A. Farias, M.V. Milošević, *J. Appl. Phys.* **119**, 093912 (2016).
- [7] M.V. Milošević, A. Kanda, S. Hatsumi, F.M. Peeters, Y. Ootuka, *Phys. Rev. Lett.* **103**, 217003 (2009).
- [8] T. Cren, L. Serrier-Garcia, F. Debontridder, D. Roditchev, *Phys. Rev. Lett.* **107**, 097202 (2011).
- [9] L. Peng, C. Cai, *J. Low. Temp. Phys.* **183**, 371 (2016).
- [10] G.R. Berdiyrov, M.V. Milošević, S. Savel'ev, F. Kusmartsev, F.M. Peeters, *Phys. Rev. B* **90**, 134505 (2014).
- [11] A. Andronov, I. Gordion, V. Kurin, I. Nefedov I. Shereshevsky, *Physica C* **213**, 193 (1993).

- [12] M.V. Milošević, W. Gillijns, A.V. Silhanek, A. Libál, V.V. Moshchalkov, F.M. Peeters, *Appl. Phys. Lett.* **96**, 032503 (2010).
- [13] G.R. Berdiyrov, S.H. Yu, Z.L. Xiao, F.M. Peeters, J. Hua, A. Imre, W.K. Kwok, *Phys. Rev. B* **80**, 064511 (2009).
- [14] G. Carapella, P. Sabatino, C. Barone, S. Pagano, M. Gombos, *Sci. Rep.* **6**, 35694 (2016).
- [15] Q. Du, *Phys. Rev. B* **46**, 9027 (1992).
- [16] T.S. Alstrøm, M.P. Sørensen, N.F. Pedersen, S. Madsen, *Acta Appl. Math.* **115**, 63 (2011).
- [17] N.B. Kopnin, *Theory of Nonequilibrium Superconductivity*, Clarendon Press, Oxford 2001, p. 213.
- [18] G.R. Berdiyrov, M.V. Milošević, M.L. Latimer, Z.L. Xiao, W.K. Kwok, F.M. Peeters, *Phys. Rev. Lett.* **109**, 057004 (2012).